7th OpenFOAM Workshop
Center of Smart Interfaces,
Technische Universität Darmstadt,
Germany
25-28 June, 2012

OpenFOAM® Implementation of an Incompressible Eddy Viscosity Turbulence Model with Zero Wall Boundary Condition Elliptic Relaxation Function

Mirza Popovac[*‡1] **and Peter Benovsky**[2]

[1,2] AIT Austrian Institute of Technology, Energy Department
Giefinggasse 2, 1210 Vienna, Austria

May 14, 2012

The $\zeta - f_0$ turbulence model, wall-bounded turbulent flows.

1. Introduction

The number of application areas of Computational Fluid Dynamics (CFD) and the complexity level of engineering problems it can handle is constantly increasing. CFD became a very powerful tool for the analysis of numerous engineering problems that involve fluid and multi-phase flows, or heat and mass transfer - to name just a few areas. Because of this wide use, for most of the commercial CFD vendors the stability and robustness of the numerical simulation are the most important requirements, for the sake of which the accuracy of the numerical predictions is sometimes sacrificed.

When it comes to the turbulence models implemented in most widely used CFD packages, owing to their numerical stability and robustness the most popular are the two-equation eddy-viscosity models: $k-\epsilon$ (Jones and Launder, 1972) and $k-\omega$ (Wilcox, 1998), together with their modifications (e.g. RNG $k-\epsilon$ and $k-\omega$ SST). Although in the past many advanced turbulent models have been proposed, ranging from the full Reynolds stress model (Launder et al., 1975) to the $\overline{v^2}-f$ elliptic-relaxation eddy-viscosity model (Durbin, 1991), for complex engineering problems they are seldom used because of the concerns about their numerical stability and computational demands.

The model of turbulence presented in this paper is based on Durbin's $\overline{v^2}-f$ idea, because it brings improvements in the quality of results (compared e.g. to the standard $k-\epsilon$ model) without having to solve too many additional transport equations (six in the case of RSM). However, while $\overline{v^2}-f$ model captures the most important near-wall flow effects, it proved to cause numerical instabilities, especially in the

‡Corresponding Author: Mirza Popovac (Mirza.Popovac@ait.ac.at)

calculations on meshes of poor quality (which are typical for complex wall-bounded engineering problems). Aiming at improving the robustness and computational stability of Durbin's original model, the $\zeta-f$ model was derived by Hanjalić and Popovac (2004) by introducing the dimensionless turbulent velocity scale ζ in the definition of the kinematic eddy-viscosity:

$$\nu_t = C_\mu k \zeta T \tag{1}$$

where $\zeta = \overline{v^2}/k$ is the ratio between $\overline{v^2}$ the fluctuating velocity component normal to the streamlines and k the turbulent kinetic energy, $C_\mu = 0.22$ is the turbulent viscosity constant, and T is the turbulent time scale.

Two groups of researchers (Hanjalić et al., 2004, and Laurence et al., 2005), independently of each other, pursued the idea of the transport equation for the normalized velocity scale ζ as an appropriate near-wall velocity scale for the turbulent viscosity (Eq.1). The outcome of this work was the model which proved to be very robust and stable, in addition to its improved accuracy in respect to the standard $k-\epsilon$ model (Hanjalić et al., 2005). In the original $\zeta-f$ model, however, the elliptic-relaxation function has a non-zero wall boundary condition, and this can become an issue when considering the implementation of this model into a general purpose RANS-based CFD fluid flow solver. In that view, this paper presents the model details and OpenFOAM® implementation of the original $\zeta-f$ model, as well as its modification so that the zero wall boundary condition for the relaxation function $f_w = 0$ is obtained. In order to distinguish between these two variants, the name $\zeta-f_0$ is proposed here for the modified model with zero wall boundary condition.

This paper is organized in five sections: after this introductory section, the second one brings the details of the proposed elliptic relaxation model, the third section shows the implementation of this model into OpenFOAM®, in the section four follows the presentation of the results obtained using the previously described procedure, as well as their comparison with the reference data, and finally the conclusions are given at the end of this paper.

2. Turbulence model

In the framework of Durbin's elliptic-relaxation eddy-viscosity turbulence modeling (of which both $\zeta-f$ and $\zeta-f_0$ models are robust variants) the anisotropy of the Reynolds stress tensor in the wall-normal direction is accounted for through the wall-normal fluctuating velocity component $\overline{v^2}$ used as the velocity scale in the definition of the turbulent viscosity ν_t (Eq.1). This approach requires extra equations to be solved, in addition to those for the turbulent kinetic energy k and the turbulent kinetic energy dissipation rate ϵ :

$$\begin{aligned} \frac{\partial k}{\partial t} + U_i \frac{\partial k}{\partial x_i} &= P_k - \epsilon + \frac{\partial}{\partial x_j}\left[\left(\nu + \frac{\nu_t}{\sigma_k}\right)\frac{\partial k}{\partial x_j}\right] \\ \frac{\partial \epsilon}{\partial t} + U_i \frac{\partial \epsilon}{\partial x_i} &= \frac{C'_{\epsilon 1} P_k - C_{\epsilon 2}\epsilon}{T} + \frac{\partial}{\partial x_j}\left[\left(\nu + \frac{\nu_t}{\sigma_\epsilon}\right)\frac{\partial \epsilon}{\partial x_j}\right] \end{aligned} \tag{2}$$

where $P_k = \nu_t S^2$ is the production of the turbulent kinetic energy, $S = \sqrt{2 S_{ij} S_{ij}}$ is the modulus of the mean rate-of-strain tensor, $\sigma_k = 1.0$ and $\sigma_\epsilon = 1.3$ are the turbulent Prandtl numbers, the near-wall damping $C'_{\epsilon 1} = C_{\epsilon 10}\left(1 + C_{\epsilon 11}/\zeta\right)$ (with $C_{\epsilon 10} = 1.4$ and

$C_{\epsilon 11}=0.012$ as model constants) being introduced for the $\zeta - f_0$ model integration to the wall, and $C_{\epsilon 2}=1.9$ being the model constant. For the turbulent kinetic energy the zero wall boundary condition applies $k_w=0$, whereas the standard wall boundary condition for the dissipation rate is expressed in terms of *k* and the wall distance (denoted as "*y*") which are evaluated in the center of the near-wall cell (denoted with the subscript "*P*"): $\epsilon_w=2\nu k_P/y_P^2$.

Durbin (1991) derived the transport equation for the wall-normal fluctuating velocity component $\overline{v^2}$ from the transport equation for the Reynolds stress component $\overline{u_i u_j}$ in the direction normal to the wall: by putting $i=j=2$ one defines $\overline{u_2 u_2}=\overline{v^2}$ which is in a general case assumed to be normal to the streamlines rather then normal to the wall boundaries. From the definition of $\overline{v^2}$ and the no-slip requirement follows the zero wall boundary condition $\overline{v^2}_w=0$. Finally, Lien and Kalitzin (2001) proposed the expansion of Durbin's original transport equation for $\overline{v^2}$ in order to obtain the zero wall boundary condition for the relaxation function f :

$$\frac{\partial \overline{v^2}}{\partial t}+U_i\frac{\partial \overline{v^2}}{\partial x_i}=kf-\epsilon\frac{\overline{v^2}}{k}N_{\overline{v^2}}+\frac{\partial}{\partial x_j}\left[\left(\nu+\frac{\nu_t}{\sigma_{\overline{v^2}}}\right)\frac{\partial \overline{v^2}}{\partial x_j}\right] \tag{3}$$

where all unclosed terms from the starting transport equation for the Reynolds stress $\overline{u_2 u_2}$ are modeled through f the relaxation function, and $N_{\overline{v^2}}$ is the model constant which is to be defined from the zero boundary condition $f_w=0$.

The first additional transport equation (further to the k and ϵ equations), which needs to be solved in the framework of this elliptic relaxation model, is the one for the normalized velocity scale ζ . The derivation of this transport equation follows from its definition: it is obtained by combining the transport equations for k (Eq.2) and $\overline{v^2}$ (Eq.3):

$$\frac{\partial \zeta}{\partial t}+U_i\frac{\partial \zeta}{\partial x_i}=f-\frac{\zeta}{k}\left[P_k-(1-N_\zeta)\epsilon\right]+\frac{\partial}{\partial x_j}\left[\left(\nu+\frac{\nu_t}{\sigma_\zeta}\right)\frac{\partial \zeta}{\partial x_j}\right]+\underbrace{2\frac{\nu+\nu_t}{k}\frac{\partial \zeta}{\partial x_j}\frac{\partial k}{\partial x_j}}_{X\approx 0} \tag{4}$$

where $\sigma_\zeta=1.2$ is the turbulent Prandtl number, and X is the cross-diffusion term omitted in order to keep the standard form of the transport equation (Popovac (2006) presented arguments that justify the omitting). From the definition of ζ the no-slip requirement at the wall yields $\zeta_w=0$ the zero wall boundary condition.

While the ζ provides viscous dumping, the relaxation function f accounts for the pressure-rate-of-strain effects (wall echo). The relaxation function f is obtained by solving the elliptic equation of Helmholtz type, as Durbin noted that the kernel of the Poisson equation of the fluctuating pressure is actually a Green's function for the modified Helmholtz equation. Hence, the solution of the elliptic equation, with the appropriate pressure-rate-of-strain model as a source term, is the model for the pressure-rate-of-strain effects.

In principle any model for the pressure-rate-of-strain terms can be used. In the present work, however, SSG (Speziale et al., 1991) was adopted for the rapid part, and RI for the slow part (Rotta, 1951). In the conjunction with the Eq.(4) the final form of the elliptic equation for the relaxation function f is constructed:

$$L^2\frac{\partial^2 f}{\partial x_i^2}-f=\frac{1}{T}\left[\left(C_{f1}-1+C_{f2}\frac{P_k}{\epsilon}\right)\left(\zeta-\frac{2}{3}\right)+\zeta\left(N_\zeta-1\right)\right] \tag{5}$$

where the model constants are $C_{f1}=1.4$ and $C_{f2}=0.65$.

The above Eq.(5) is the second additional equation to be solved in the framework of the $\zeta-f_0$ model, with its wall boundary condition defined as:

$$f_w=(N_\zeta-2)\frac{2\nu\zeta_P}{y_P^2} \tag{6}$$

where N_ζ is the model constant which can be selected in order to adjust the f wall boundary condition.

The final set of equations of the present elliptic relaxation model is given by Eqs.(1), (2), (4), (5), (6) and (7). Clearly, by choosing $N_\zeta=2$ the zero wall boundary condition is obtained $f_w=0$, and this arrangement will be named the $\zeta-f_0$ model. On the other hand, with $N_\zeta=1$ the obtained set of equations is the original $\zeta-f$ model as derived by Hanjalić and Popovac (2004). The subscript "*0*" used for the distinction between the parent $\zeta-f$ model and the present $\zeta-f_0$ modification, to stresses the point that the zero wall boundary condition holds for the additional turbulent quantities in this model, and not to denote a new variable.

In order to complete the $\zeta-f_0$ set of equations, the time scale T and length scale L have to be defined. To prevent singularities that could occur in Eq.(2), and Eq. (5) (which could cause the unrealistic behavior of turbulent quantities) T and L are limited by the respective Kolmogorov values from below, and the realizability constraints limit them from above:

$$\begin{aligned} T&=max\left[min\left(\frac{k}{\epsilon}\,,\,\frac{C_T}{\sqrt{6}C_\mu|S|\zeta}\right),C_\tau\left(\frac{\nu}{\epsilon}\right)^{1/2}\right]\\ L&=C_L max\left[min\left(\frac{k^{3/2}}{\epsilon}\,,\,\frac{k^{1/2}}{\sqrt{6}C_\mu|S|\zeta}\right),C_\eta\left(\frac{\nu^3}{\epsilon}\right)^{1/4}\right] \end{aligned} \tag{7}$$

where ν is the kinematic molecular viscosity of the fluid, and $C_T=0.6$, $C_\tau=6.0$, $C_L=0.36$ and $C_\eta=85$ are the model constants. The whole set of constants for the $\zeta-f_0$ model is summarized in Table 1. Note that the coefficients used for the $\zeta-f_0$ model are left identical to those of its parent $\zeta-f$ formulation, although some fine tuning of the model coefficients might have been used to improve the predictions.

Final remark in this section, presenting turbulence model, is concerning the explanation for the robust computational behavior of the $\zeta-f_0$ model. It is not only the zero wall boundary condition for the turbulent quantities that improves the robustness, but also the bounded values for ζ (from the definition follows mathematical inequality $0\le\zeta\le2$ which is physically even stronger), and the near-wall balance of the source terms in the ζ transport equation (only f and the diffusion of ζ are making the balance very close to the wall).

3. Implementation of the model

The following paragraphs present the details of the OpenFOAM® implementation of the model described above. In this work already existing RNG $k-\epsilon$ implementation in OpenFOAM® served as the base of the implementation, since here two additional transport equations need to be solved for ζ and f , together with two volumetric scalars for T and L . The starting point for the implementation of the $\zeta-f_0$ model into any RANS-based CFD fluid flow solver is the generic transport equation of the

standard form, which for an arbitrary passive scalar ϕ (such as the additional turbulent quantity) can be written as:

$$\underbrace{\frac{\partial \phi}{\partial t}}_{Local} + \underbrace{\nabla \cdot (\boldsymbol{U} \phi)}_{Convection} - \underbrace{\nabla \cdot (\Gamma_\phi \nabla \phi)}_{Diffusion} = \underbrace{S_\phi}_{Source} \tag{8}$$

In the generic transport equation of the standard form (the same form e.g. for the k and ϵ transport equations) there are four terms (Eq.8): the local rate of change which is activated for the unsteady flow calculations only, the convection for which the convective scheme is of decisive importance, the diffusion for which the diffusivity coefficient Γ_ϕ needs to be defined, and finally the source term S_ϕ on the right hand side of the equation. In OpenFOAM® the implementation of such a transport equation is very easy, with the syntax written as:

```
solve
(
    fvm::ddt(phi)                  // Local change
  + fvm::div(phi, phi)             // Convection
  - fvm::laplacian(Gamma, phi)     // Diffusion
  ==
    S_phi                          // Source term
);
```

In order to analyze the individual terms of transport equations for two additional volumetric scalars, needed for the $\zeta - f_0$ model, Eq.(8) has to be re-casted into the form given by Eq.(4) and Eq.(5) (for ζ and f respectively). In the case of the equation for ζ (Eq.4), this means that the effective viscosity is specified for the diffusivity coefficient $\Gamma_\zeta = \nu + \nu_t / \sigma_\zeta$. Specific for the equation for f (Eq.5) is that it does not contain the local rate of change term nor the convection term. Furthermore, comparing Eq.(8) and Eq.(5) it can be concluded that the turbulent length scale squared L^2 is the diffusivity coefficient in the f equation. However, in the actual implementation of the model the entire f equation is divided by L^2 (since it stays outside of the Laplacian), so the actual diffusivity coefficient for f is set to unity and L^2 is transferred into the source term S_f .

The implementation of source terms, given by Eq.(9) and Eq.(10), can be done either implicitly (denoted as *Su*) or explicitly (denoted as *SuSp*). The explicit part is the RHS of the transport equation, while the implicit part is definded by its partial derivative with respect to that solution variable. In this respect, in the context of the $\zeta - f_0$ model, the source terms for ζ read:

$$\begin{aligned} Su(\zeta) &= f - \frac{\zeta}{k}\left(P_k + \epsilon\right) \\ SuSp(\zeta) &= -\frac{1}{k}\left(P_k + \epsilon\right) \end{aligned} \tag{9}$$

and for f these are:

$$Su(f) = \frac{1}{L^2}\left\{\frac{1}{T}\left[\left(C_{f1} - 1 + C_{f2}\frac{P_k}{\epsilon}\right)\left(\zeta - \frac{2}{3}\right) + \zeta\right] + f\right\} \tag{10}$$

$$SuSp(f)=\frac{1}{L^2}$$

which follows directly from Eq.(4) and Eq.(5).

To conclude the discussion about the $\zeta-f_0$ model implementation, there are two remarks. Firstly, it was already mentioned that in the present implementation the entire f equation (Eq.5) is divided by L^2 (Eq,10), and consequently the diffusivity coefficient in the f equation is set to unity. Therefore it is important, from the numerical point of view, to prevent the turbulent length scale L becoming zero (the same like with the turbulent time scale T). And secondly, further to the initial conditions for k and ϵ , which are well established (e.g. through the turbulent intensity and the viscosity ratio), the initial conditions for ζ and f are also very simple. Since zero boundary condition at the wall applies for f (Eq.6), it is reasonable also to initialize the f field with zero. As for the normalized velocity scale, in the equilibrium state (when the $\zeta-f_0$ model reduces to the standard $k-\epsilon$ model) ζ obtains the value $2/3$ and hence $\zeta_{init}=2/3$ is a good recommendation for the ζ initialization.

4. Test cases

In order to test the performance of the presented turbulence model, the simulations of several generic turbulent test flows were performed: the fully developed turbulent plane channel flow, the backward facing step and the circular impinging jet (Fig.1). The predictions of these well documented test cases reveal the capability of this elliptic relaxation model to capture the basic wall-related flow effects.

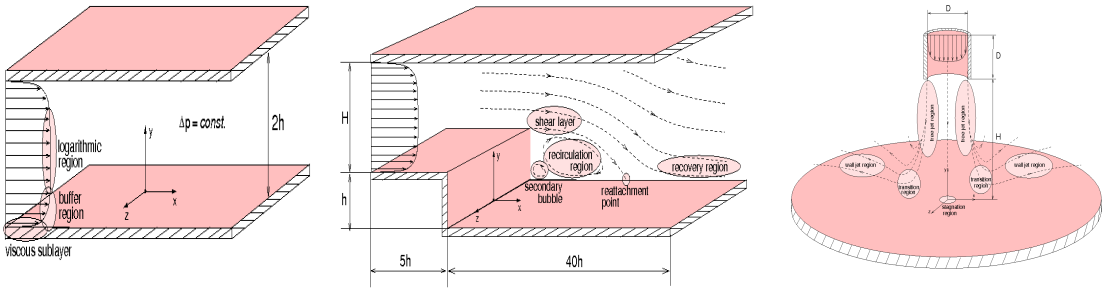

Figure 1: flow geometry sketch for the plane channel (left), backward facing step (middle) and circular impinging jet (right), with the main flow characteristics.

The basic wall-bounded flow case for testing turbulence models is a fully developed turbulent flow between two parallel plates (Fig.1 left). Due to its simplicity, this flow case has been thoroughly investigated in the past, both experimentally and numerically . For the comparison, in the present study the Reynolds number was $Re_\tau=5000$ based on the friction velocity and h the channel half height (Tanahashi et al., 2004), and the mesh used was sufficiently fine to resolve the viscous sublayer.

For the flow with massive separation, the testing was performed on the backward facing step configuration (Fig.1 middle). In the literature one can find results both from experimental and numerical investigations of this test case for various flow

configurations (different H/h height-to-step ratios). The results presented here are compared with the experimental results of Vogel and Eaton (1985), with the Reynolds number based on the step height Re_h=28000 and H/h=4 for selected geometry configuration.

The stream of flow impinging onto the target plate is often encountered in different engineering applications due to its high heat transfer coefficient (Fig.1 right). Therefore various geometry configurations of this generic flow (different H/D ratios of distance-to-diameter) have been thoroughly investigated both experimentally and numerically. The test case analyzed here, with the Reynolds number based on the pipe diameter Re_D=23000 and H/D=2 geometry configuration, is compared with the experimental data of Baughn and Shimizu (1992) and Baughn et al. (1992).

4.1 Fully developed turbulent plane channel flow

As Fig.2 shows, for fully developed turbulent plane channel flow, very good agreement between the $\zeta-f_0$ predictions and the DNS results holds both for the mean velocity and turbulent quantities. The results are obtained both with the integration to the wall (ItW) and wall function approach (WF), which was enabled by defining the $\zeta-f_0$ model with the zero wall boundary conditions for additional turbulent quantities. At this point it is important to note that the $\zeta-f_0$ model was originally developed as a low-Re model for wall-bounded flows. Hence the behavior of the model in the wall vicinity is of the decisive importance.

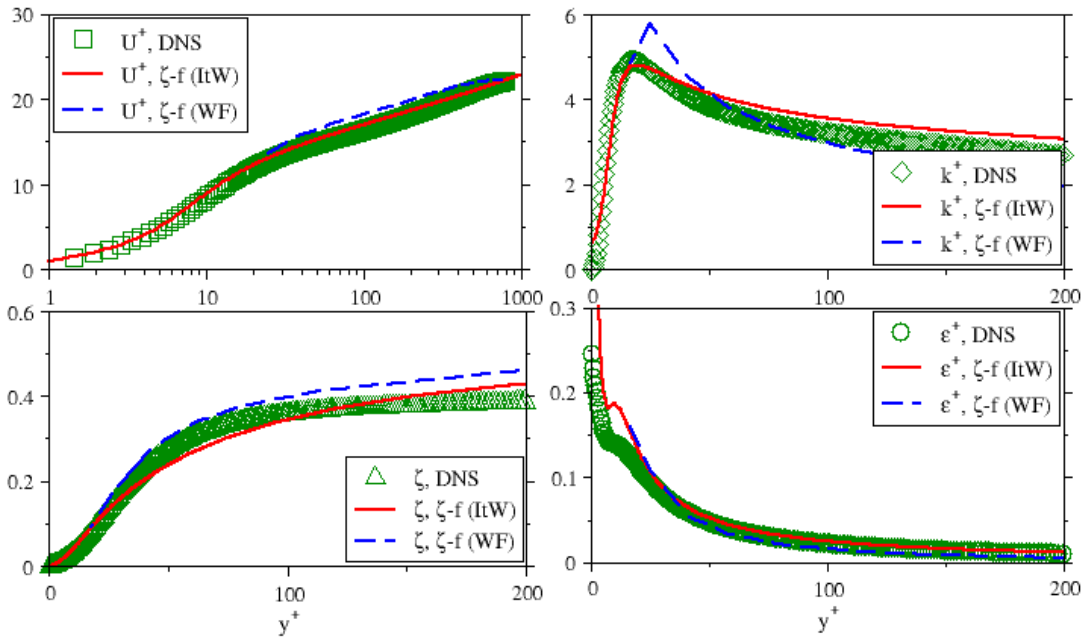

Figure 2: profiles of the streamwise velocity, normalized turbulent fluctuating velocity, turbulent kinetic energy and dissipation rate, obtained with the mesh suited for the integration to the wall and wall function (DNS: symbols, lines: $\zeta-f$ model).

4.2 Backward facing step flow

As shown in Fig.3, the backward facing step flow results obtained with the $\zeta-f_0$ model are in very good agreement with the measurements of Vogel and Eaton. For the quantitative comparison between the reference data and the $\zeta-f_0$ predictions, the velocity magnitude show that the main flow features (shear layer, recirculation and recovery region) are properly captured. The same cannot be concluded for the results obtained with the $k-\epsilon$ model, which under-predict the recirculation zone.

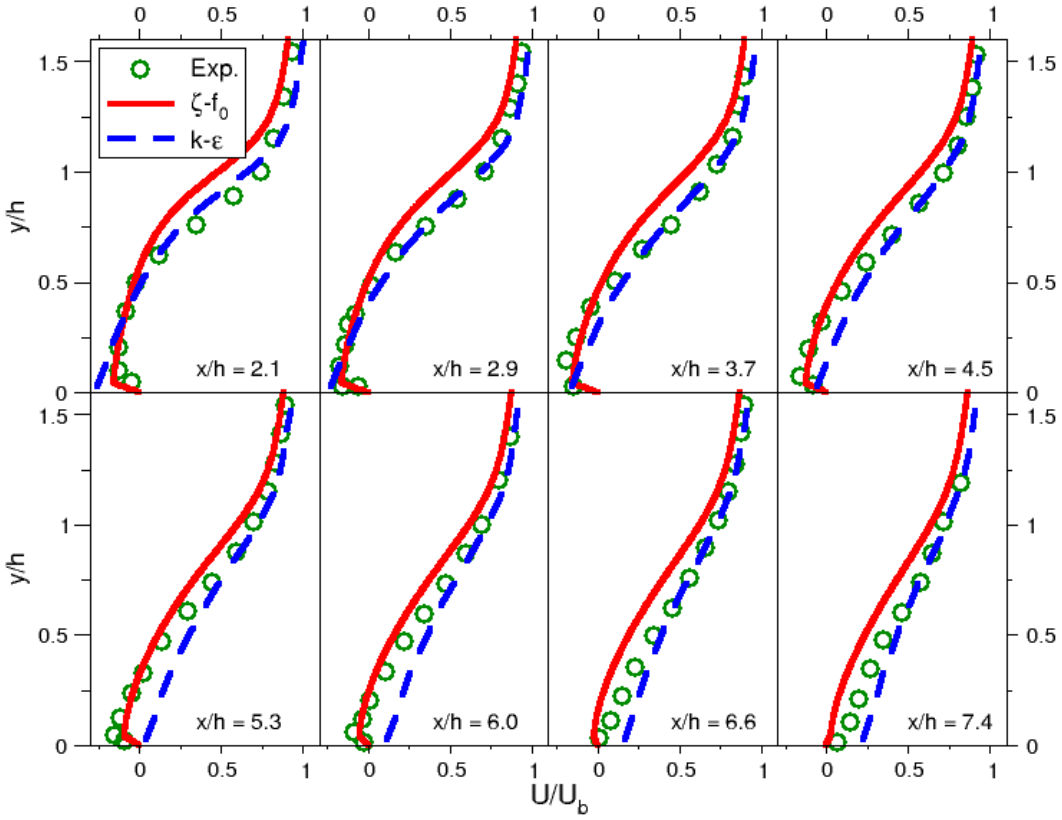

Figure 3: the profiles of the streamwise velocity component normalized with the bulk velocity, obtained with the $\zeta-f_0$ model for the backward facing step flow (experiment: symbols, lines: $\zeta-f_0$ and $k-\epsilon$ model).

4.3 Circular impinging jet flow

From the quantitative comparison between the $\zeta-f_0$ results and the experiments, shown in Fig.4 (Baughn et al., 1991), one can see that the spreading of the jet issued from a circular pipe is very well captured (unlike too diffusive flow pattern predicted by the $k-\epsilon$ model). The flow pattern characteristic for the impinging jet, shown in Fig.5 by the contour plots of the velocity magnitude and the turbulent kinetic energy (the stagnation point, free jet, transition and wall jet regions) can be clearly identified. But even more importantly, the over-prediction of the turbulent kinetic energy in the

stagnation region (characteristic for the $k-\epsilon$ model) is eliminated with the $\zeta-f_0$ model.

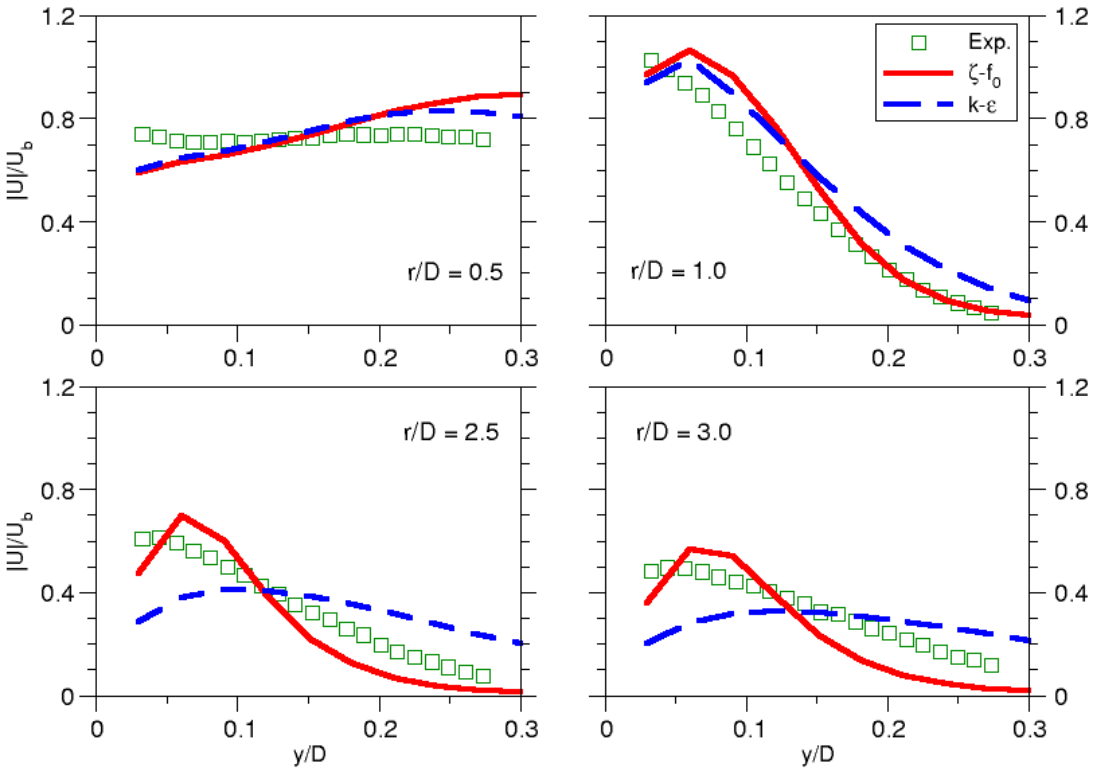

Figure 4: the profiles of the velocity magnitude normalized with the jet bulk velocity, obtained with the $\zeta-f_0$ model for the circular impinging jet flow (experiment: symbols, lines: $\zeta-f_0$ and $k-\epsilon$ model).

5. Conclusions

The aim achieved by the derivation of the $\zeta-f_0$ model is defining of the robust elliptic-relaxation eddy-viscosity turbulence model whose easy implementation in OpenFOAM® is simple and straightforward, so that this "upgrade" of standard $k-\epsilon$ model is fully justified for the simulations of complex wall-bounded flows. Namely, the parent $\zeta-f$ version of this novel model proved to be computationally robust and stable, with the quality of the results superior to the models widely used (e.g. $k-\epsilon$ or $k-\omega$ model). With the $\zeta-f_0$ model, however, the implementation into a general purpose RANS-based CFD code is very simple and straightforward, because the form of the additional equations being solved is identical to those already existing in the given code, and the zero wall boundary condition for the additional turbulent quantities is the simplest possible to implement. Hence, with the $\zeta-f_0$ model there is a minimal programing effort required in order to have all the advantages of the advanced elliptic-relaxation turbulence modeling concept for the numerical analysis of complex engineering flows.

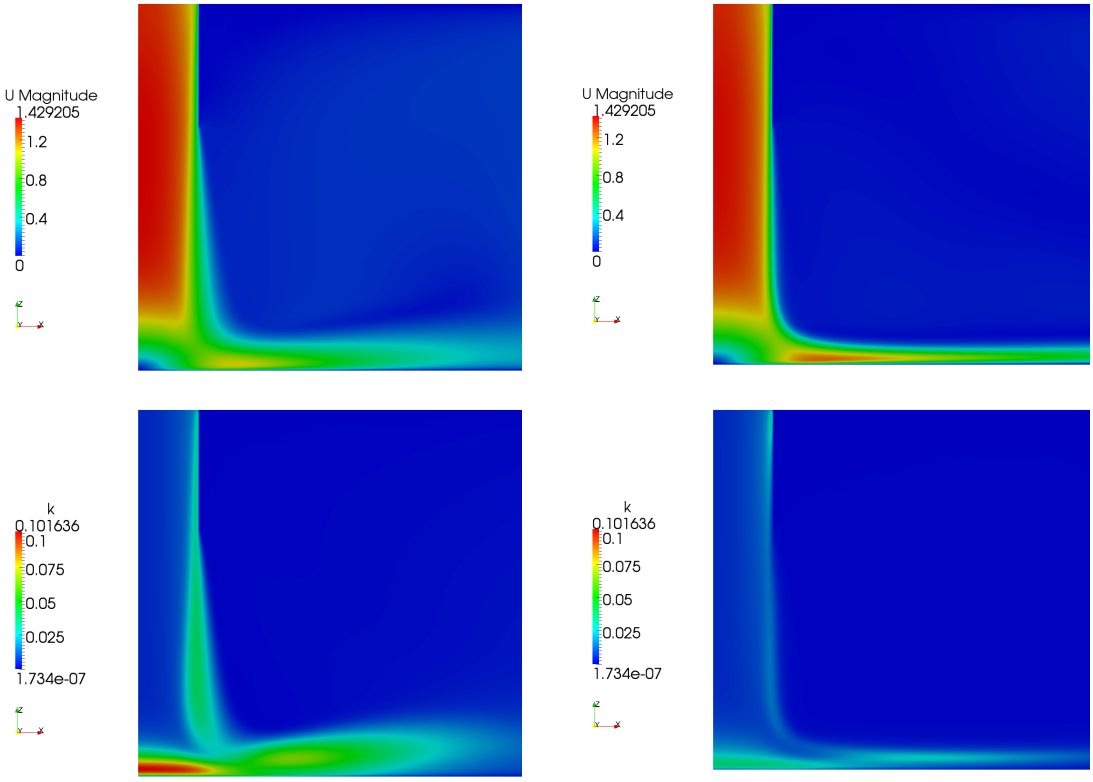

Figure 5: the comparison between the $k-\varepsilon$ (left) and $\zeta-f_0$ (right) results for impinging jet flow (above: velocity magnitude, below: the turbulent kinetic energy).

The implementation of the $\zeta-f_0$ model is based on the existing OpenFOAM® implementation of the RNG $k-\epsilon$ model. This implementation implies the use of two additional volumetric scalars, for which the transport equations are solved. In both equations the diffusivity coefficient has to be calculated, and the required source terms have to be defined. The convection term and the local rate of change have to be appropriately chosen, and zero constant value boundary conditions specified at all walls. Finally, additional two volumetric scalars have to be defined for the realizable length and time.

The flow predictions and the computational performance of the $\zeta-f_0$ model was tested on several flow cases. Firstly, the computation of the generic flow cases was performed (the fully developed turbulent plane channel flow, the backward facing step and the round impinging jet), and the obtained results are in good agreement with the reference data. And secondly, as the example of the complex wall-bounded flows of engineering relevance, the wall-mounted cubes cooled simultaneously by a cross-flow and a jet was calculated. The accuracy of the results obtained with the $\zeta-f_0$ model are very good, particularly in comparison with the standard $k-\epsilon$ model. The only drawback of this "upgrade" to the $\zeta-f_0$ model is approximately 30% increase in the computation time, which is definitely much less then the increase one would expect (100% more compared to the standard $k-\epsilon$ model, since two additional equations are solved). Therefore the price paid in increased computational demand is worth the increased quality of the results.

REFERENCES

1. Jones, W. P. and Launder, B. E. (1972). The prediction of laminarization with a two-equation model of turbulence. *Int. J. Heat Mass Transfer*, 15, pp. 301-314.
2. Wilcox, D.C. (1998). *Turbulence Modeling for CFD*. DCW Industries, Inc., La Canada, California.
3. Launder, B.E., Reece, G.J. and Rodi, W. (1975). Progress in the Development of a Reynolds-Stress Turbulence Closure. *J. Fluid Mech.*, 68(3), pp. 537-566.
4. Durbin, P.A. (1991). Near-wall turbulence closure modelling without damping functions. *Theor. Comput. Fluid Dyn.*, 3, pp. 1–13.
5. Hanjalić, K., Popovac, M. and Hadžiabdić, M. (2004). A robust near-wall elliptic-relaxation eddy-viscosity turbulence model for CFD. *Int. J. Heat and Fluid Flow*, 25/6, pp. 1047-1051.
6. Laurence, D., Uribe, J. and Utyuzhnikov, S. (2005). A robust formulation of the v2−f model. *Flow Turbulence Combustion*, 73, pp. 169-185.
7. Hanjalić, K., Laurence, D., Popovac, M. Uribe, J. (2005). Impinging jet cooling of wall mounted cubes. In W Rodi & M Mulas (Eds.), *Proceeding of ERCOFTAC International symposium of engineering turbulence modelling and measurements* (ETMM6), Sardinia, Italy, pp. 67-76.
8. Lien, F.S. and Kalitzin, G. (2001). Computations of transonic flows with the v2-f turbulence model, *Int. J. Heat Fluid Flow*, 22, pp. 53-61.
9. Popovac, M. (2006). *Modelling and simulation of turbulence and heat transfer in wall-bounded flows*, Ph.D. thesis, Delft University of Technology, Delft, The Netherlands.
10. Speziale, C.G., Sarkar, S. and Gatski, T.B. (1991). Modeling the pressure strain correlation of turbulence: an invariant dynamical systems approach, *J. Fluid Mechanics*, 227, pp. 245–272.
11. Rotta, J.C. (1951). Statistische Theorie Nichthomogener Turbulenz. *Z. Phys.*, pp. 129, 547.
12. Tanahashi, M., Kang, S.-J., Miyamoto, T., Shiokawa, S. and Miyauchi, T. (2004). Scaling law of fine scale eddies in turbulent channel flows up to Re_τ=800. *Int. J. Heat and Fluid Flow*, 25/3, pp. 331-340.
13. Vogel, J.C. and Eaton, J.K. (1985). Combined heat transfer and fluid dynamic measurements downstream of a backward-facing step, *ASME J. Heat Transfer*, 107, pp. 922–929.
14. Baughn, J. and Shimizu, S. (1989). Heat transfer measurements from a surface with uniform heat flux and an impinging jet, ASME J. Heat Transfer, 111, pp. 1096–1098.
15. Baughn, J.W., Hechanova, A.E. and Yan, X. (1991). An experimental study of entrainment effects on the heat transfer from a flat surface to a heated circular impinging jet, *J. Heat Transfer*, 113, pp. 1023–1025.